Case study in NW Greece of passive seismic tomography: a new tool for hydrocarbon exploration

Sotiris Kapotas[1], G-Akis Tselentis[2], Nick Martakis[3]

Introduction

We have learned more about the structure of the Earth and its crust from earthquake seismology in all its facets than from any other single geophysical or geological method. The use of the vast amount of information provided by the natural seismicity of the earth has been largely restricted to the investigation of classical seismological problems or to large scale investigations of the earth's interior, with relatively little attention being paid towards small scale hydrocarbon exploration. Listening to the earth passively, and using the collected seismological information wisely, can be successfully applied to hydrocarbon exploration, as is shown in the present investigation.

Controlled source seismology uses conventional surface sources such as vibroseis, explosives or airguns to generate seismic waves whose travel times and amplitude distribution through the earth are used to determine structural images and bulk physical properties of the subsurface. In contrast, passive seismic tomography uses micro-earthquakes as an energy source to probe earth structure.

It is a fairly simple concept, based on the fundamental principle that all small movements and 'roars' in the earth are actually seismic sources. Both compressional and shear waves are emitted from an earthquake source and can be used for independent estimates of compressional (V_P) and shear (V_S) velocities of the various geological formations.

The definition of velocity structure in a complex tectonic environment is a challenging task for conventional reflection velocity analysis based on NMO methods. In recent years, there has been an increase in exploration activity in geologically complex areas, such as fold and thrust belts, and even seeking good seismic images beneath high impedance layers such as basalt.

Exploration in these areas is challenging, as well as expensive, and is driving the oil exploration industry towards the application of state of the art techniques. A key aspect of tackling the 'complex geology' problem has been the design and implementation of new types of seismic acquisition and processing strategies. The passive seismic tomography method falls into this category.

Conventional land seismic is a labour-intensive business with expensive recording crews and set-ups of hundreds of miles of cable out on the ground, while geophones have to be deployed and retrieved manually. Surface access is needed for vibrators and shot-hole rigs, while permitting and other environmental issues mean high costs.

The rationale for the application of passive tomography as a complementary imaging tool is multifold.

It is a cost effective manner to image a large area where the terrain is difficult (mountainous or even shallow water) and, as a consequence, conventional seismic is expensive and may be of poor quality.

Since the seismic energy from microearthquakes comes from below the target of interest (Fig.1) it can be easily used to map complex tectonic regions (i.e. overthrust belts, sub-basalts, shallow carbonates etc.) characterised by seismic energy penetration problems.

Another advantage of passive seismic tomography is the capability to measure accurately an intrinsic V_P/V_S ratio.

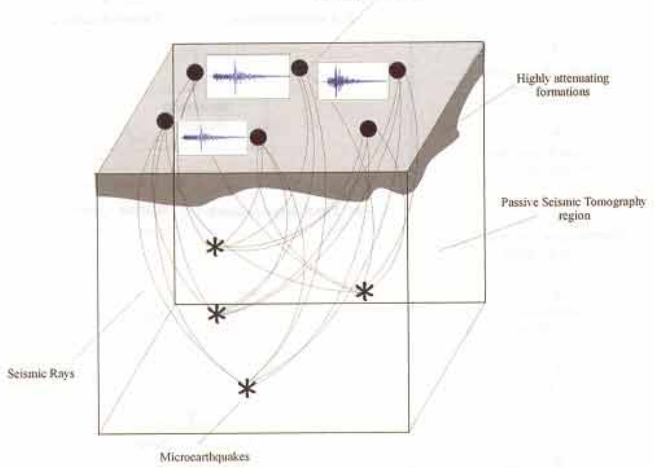

Figure 1 *Principles of 3-D Passive Seismic Tomography. The seismic sources (naturally occurring microearthquakes) are beneath the target.*

[1] *formerly TOTAL SA, now at Landtech Enterprises SA, Ocean House, Hunter St., Cardiff Bay, CF10 5FR, UK (E-mail: sotiris.kapotas@landtech.org)*
[2] *University of Patras, Seismological Laboratory, 22500 Rio, Greece (E-mail to: tselenti@upatras.gr)*
[3] *Landtech Enterprises SA, 16 Kifisias Ave., 15125, Marousi, Athens, Greece (E-mail: nmartakis@landtech.org)*

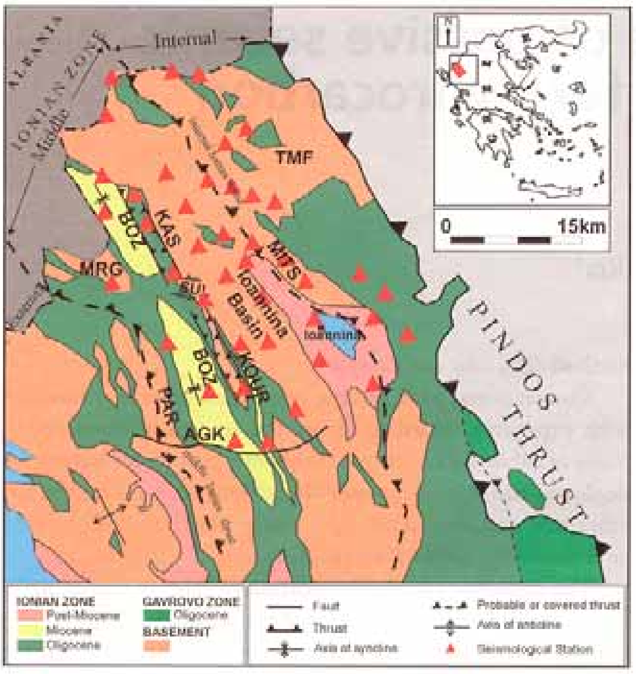

Figure 2 *The main geotectonic features of the project area. Red triangles depict the seismological stations.*

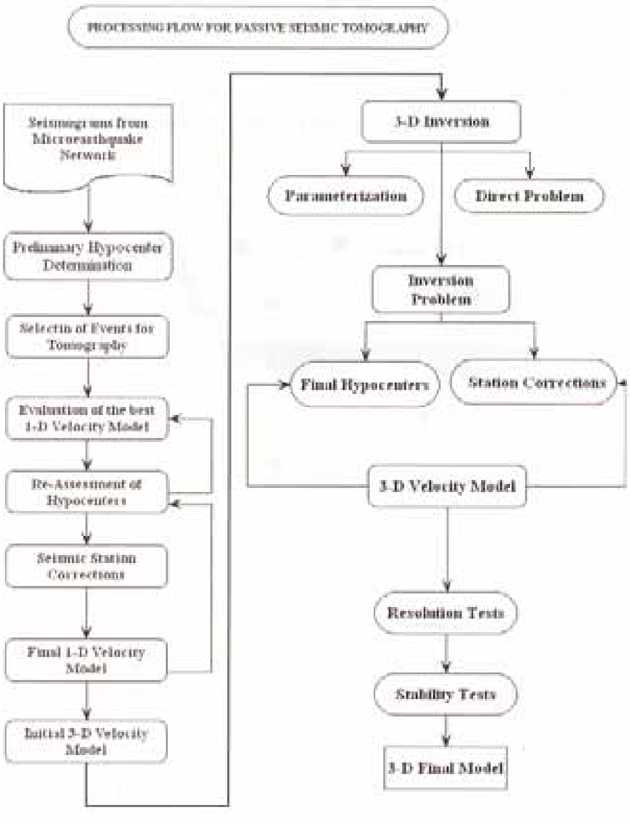

Figure 3 *General processing flow of passive seismic tomography.*

This is a direct consequence of the production of high amplitude shear waves by small earthquakes that are reliably recorded by (3-component) surface receivers. In contrast, 3D reflection seismic methods employ man-made sources (e.g. explosions) that do not produce large shear waves, so that detecting and identifying the weak shear waves reflected deep in the medium is not generally reliable, and often not even possible. Consequently, the active seismic reflection methods currently employed by the petroleum industry do not adequately provide material parameter information related to the shear velocities in the medium.

Typically, a passive seismic 3D survey will cost less than a conventional 2D survey by several orders of magnitude. Drilling and explosives, for example, generally account for almost half of conventional 3D seismic cost. These costs are eliminated with passive seismic. Furthermore, the recording station density required in this methodology is significantly less, meaning significantly smaller equipment inventory and crew size. A passive seismic crew will be normally five to 10 people, compared with a conventional crew that will number upwards of 50.

Another important aspect of the technique is that it has the advantage of being environmentally friendly. The absence of explosives and heavy vehicle support for conventional sources permits activity in terrains that might otherwise be inaccessible, and almost eliminates any environmental issues.

In the following sections we present a successful application of passive seismic tomography for hydrocarbon exploration in the area of Epirus, Greece.

Study area

Epirus is a complex tectonic environment located in the NW corner of Greece. It is the region where the transition of the extensional Inner Aegean regime to the compressional outer Aegean takes place. This transition is mapped on the basis of faulting, which varies from thrust and strike-slip to normal faults. The main structures are thrust belts that trend NNW as a result of E-W shortening. They are cut by almost perpendicular strike-slip or normal faults.

Starting from the east, the Pindos Zone is thrust onto the Gavrovo Zone, and the Gavrovo onto the Ionian Zone (Fig.2). The topographic relief of the area is very steep, resulting in extremely high costs for conventional seismic surveys. Furthermore, the karstified carbonate outcrops present serious seismic penetration problems due to strong attenuation of the seismic reflection energy.

Acquisition of passive data

A microearthquake network consisting of forty 24-bit seismic recorders with specially designed 4.5 Hz 3-component shallow borehole LandTechBHS45 seismometers (connected to LandTechAF25 preamplifiers) was installed in shallow boreholes (5-15 m) to improve S/N ratio (Fig.2). The recording system had a flat transfer function from 1-50 Hz and was synchronized via GPS. The network covered an area of about 3000 km^2 and was continuously recording for 10 months at a sampling rate of 200 Hz.

Data processing

Manipulation of the passive seismic data recorded over the entire network is not an easy task. A special neural based algorithm was designed for the automatic detection of P and S wave phases, and the sorting of the corresponding seismic wave forms — per event and per station. Next, P and S phase picking was verified manually and the data were subsequently incorporated for hypocentre and earthquake parameter calculations.

Data selection is one of the most critical and important steps to be undertaken before any passive tomographic inversion, where we solve simultaneously for earthquake location and velocity model adjustments. It is therefore important to use earthquakes with locations well constrained by the data. Around 450 earthquakes out of 900 well located events, satisfying strict selection criteria (events must lie within the network and the inversion grid, have a minimum number of recorded phases, and an upper limit in the RMS residual) resulted in a total of 13 091 phases that were included in the velocity inversion.

The joint problem for 3D velocity distribution and hypocenter locations is solved with a progressive inversion algorithm developed by LandTech, based upon the proposed methodologies of Thurber (1993), Eberhart-Phillips (1993), Zhao *et al.* (1992) and Asad *et al.* (1994). A series of linearized systems of equations relating travel time residual and adjustments in origin time, hypocentral co-ordinates and velocity parameters is solved repeatedly using damped least squares. Parameter separation is used to decouple hypocenter locations and velocity adjustments, while maintaining the mathematically coupled nature of the overall problem.

In the first step, a minimum 1D velocity model is computed. A minimum 1D velocity model with corresponding station corrections results from simultaneous inversions of a large number of travel times from selected high quality events for both model and hypocenter parameters. It is designed to locate these events with the smallest possible uniform location error.

In the second step, we invert the same dataset for 3D V_P structure and hypocenter parameters using travel time residuals all over the entire network. Model parameterization in this method assumes a continuous velocity field. The earth structure is represented in three dimensions by velocities defined at discrete points (nodes). Velocity at any intervening point is determined by linear interpolation among the surrounding eight nodes. Values at the velocity nodes are systematically perturbed during inversion. Derivative weight sum (DWS) is a useful measure of ray density in the neighborhood of a node, and is used to determine which of the nodes should be included in the inversion. DWS for a node is similar to the ray hit count, but weighted by the ray-node separation and ray path length in the vicinity of the node.

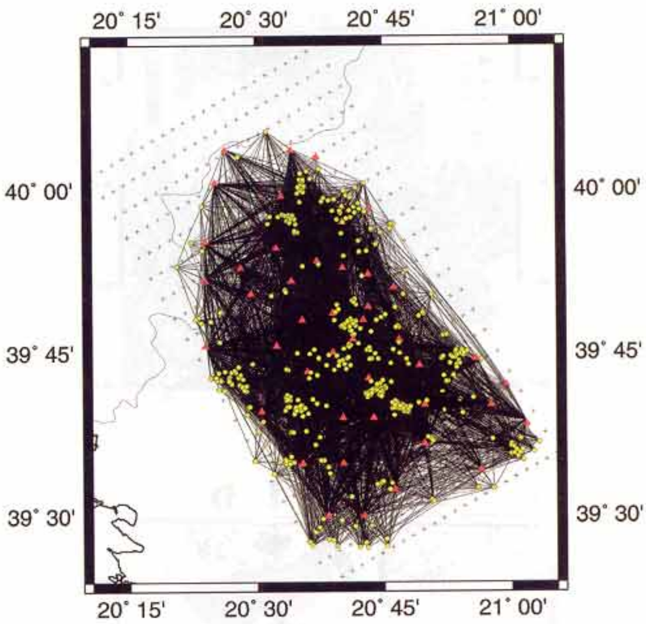

Figure 4 *Horizontal grid design for 3D tomography. Earthquakes used in the inversion are shown as small yellow circles, stations as red triangles and straight rays connecting hypocenters and stations with black lines. The positions of the grid nodes for the inversion are shown with black crosses.*

To solve the forward problem, the algorithm selects the path with the least travel time from a suite of circular arcs connecting the source and receiver. The iterative 3D ray-tracing and pseudo-bending method of Eberhart-Phillips (1993) is applied. Hypocentre locations are updated within the new velocity model at each iteration. Figure 3 presents a general processing flow followed during the present investigation to obtain the V_P and V_S 3D structure.

Considering the ray distribution of the selected data, an initial horizontal grid with 2 x 4 km node spacing covering an area of 70 x 40 km was chosen for this inversion, covering a depth range from the surface to 10 km (Fig.4). Ultimately, the grid was reduced to 0.5 x 0.5 km in areas of interest and stations were moved about to improve ray coverage. Nodes within a cell that was covered with a minimum of 10 rays were kept fixed during the inversion. With this parameterization we were able to obtain a reliable image of the 3D structure.

Resolution tests

A 3D tomographic image is only as good as its resolution estimates, so great care has to be taken to assess the resolving power of the dataset. This can be done using many different procedures and their correlation can lead to safe conclusions about the resolution power of the collected seismological data and, therefore, the quality of the tomographic inversion results. These procedures do not only verify the level of the accuracy obtained, but also point out sub-regions

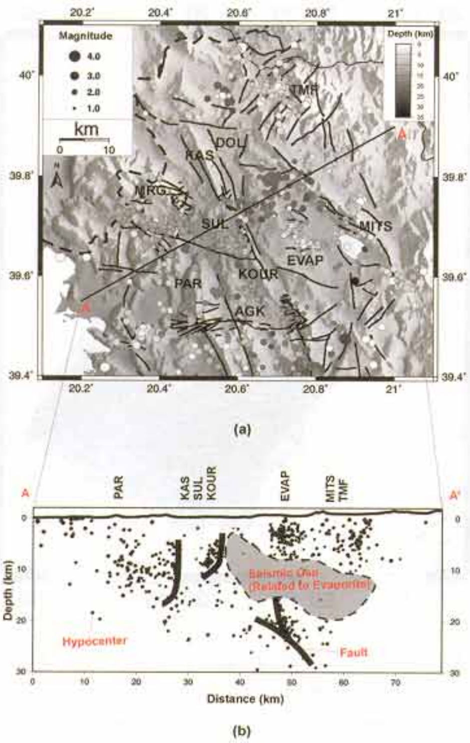

Figure 5 *(a) Optimally located microearthquakes, (b) Depth distribution of microearthquakes projected along a vertical plane passing throughout AA'. Note the absence of seismicity within the evaporite.*

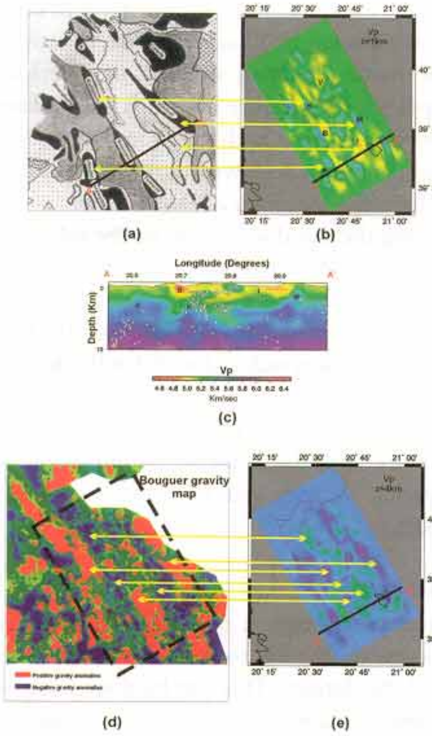

Figure 6 *(a) Main geological formations, (b) Horizontal V_P slice at 1Km depth, (c) V_P velocity cross section along AA', (d) Bouguer gravity map of the area, (e) Horizontal V_P slice at 4Km depth.*

of higher or lower analysis precision, thus making it easier to control the interpretation of the results.

One very rough estimate of the illumination of the model space is given by the hit count, which sums the number of rays that contribute to the solution at one node.

A more sensitive measure is the DWS parameter described above, since it quantifies the relative ray density in the volume of influence of a model node, weighting the importance of each ray segment by its distance from the model node.

An even better measure of estimating the quality of the inversion result is the resolution matrix (RM). Each row of RM describes the dependency of the solution for one model parameter on all the others. As a first order diagnostic tool, the diagonal elements of RM can be used, since they show the amount of independence in the solution of one model parameter.

Finally, the most practical and reliable way to verify the resolution of a Passive Tomographic Survey is the *checker board test,* as all the calculations are determined in the same way as in the original 3-D tomographic inversion. (Visit http://www.landtech.org/quality_control.htm)

The objective of this technique, in the first step, is the calculation of synthetic arrival times for the P- and S-waves (forward problem), using the same source-receiver geometry, damping factor and grid-spacing used in the 3-D inversion, together with a velocity model consisting of the 1-D initial model and 5-10% velocity anomalies superimposed on it (spike model) with known shape and position, in the target area. The second step is the reconstruction of the above-mentioned features (inverse problem) using the synthetic arrival times and the initial 1-D velocity model (without velocity anomalies). In this step, the source-receiver geometry remains the same, because we do not allow alteration of the hypocentral positions of the earthquakes in the forward solution (only the arrival times are calculated according to the synthetic velocity model).

After the 3-D inversion, the resultant velocity model is compared with the synthetic one, and from these images we can conclude where the resolving power of the dataset is able to describe already known velocity anomalies.

Results

Figure 5 presents the distribution of the recorded microearthquake epicenters all over the project area. A significant amount of the seismic energy was released rather homogeneously within the upper 10 Km of the crust. This justifies a good ray coverage of the geological formations to be investigated (Fig.4). Most of the recorded events (Fig.5a) have clear compressional (P) and shear (S) phases. Note the absence of any seismic activity within the evaporites (Fig.5b), since these formations possess no shear strength.

During integration, interpretation and prior to any well information, the inverted velocity results were assessed and evaluated by comparing and correlating features of the 3D-

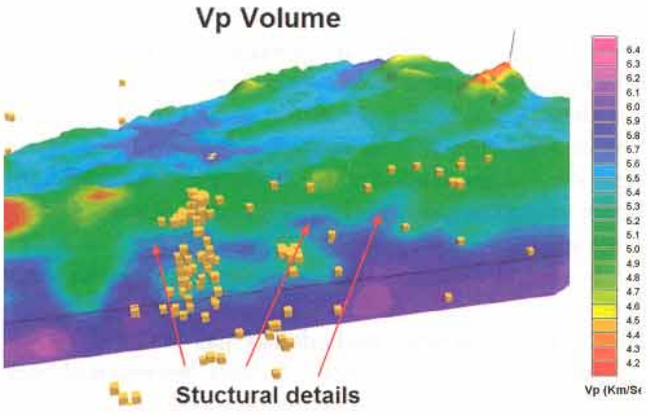

Figure 7 *3-D V_P volume of the project region showing structural details. Yellow cubes depict microearthquake hypocenters.*

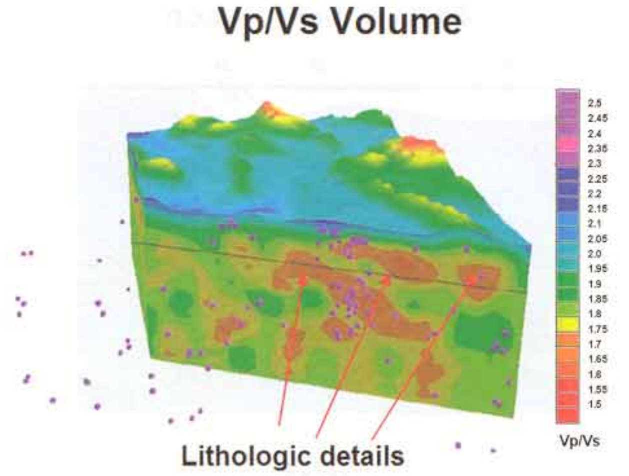

Figure 8 *3-D V_P/V_S volume of the project region showing lithologic details.*

velocity structure with other geological and geophysical observations and datasets. Velocity structure images were taken at specified vertical cross-sections and at horizontal depth slices. Special attention was paid in order to judge the reliability of the tomographic results by comparing shallow depth velocity models with the prevailing surface geology.

Figures 6a and 6b compare the surface geology to the V_P velocity structure at 1 km depth, indicating that the main topographic and geologic features are indeed present in the passive section. A cross section of the V_P model along path AA' (Fig. 6c) confirms the character of the structural features in depth in relation to the outcrops in Figure 6a.

A very important comparison has been made between the Bouguer gravity anomaly (Fig. 6d) and a V_P depth slice at 4km (Fig. 6e). The high degree of correlation from these different data sources is compelling, suggesting that all the predominant geological formations in the region are clearly depicted in the passive seismic tomography data, supporting our confidence in this new methodology.

Integration and correlation of the inverted 3-D V_P velocity (Fig. 7) and 3-D V_P/V_S (Fig. 8) tomograms were carried out for the structural and lithologic modeling of the area, helping prospect identification, and providing confidence in the overall interpretation.

By selecting specific velocity intervals from the 3-D velocity space obtained we were able to reveal various geological formations of interest such as the 3-D distribution of the evaporites (Fig. 9) and the carbonates (Fig. 10). It is notable that all surface outcrops of the evaporite structure coincide with the tomographic results.

The striking results of the passive seismic were confirmed by the well and the VSP data analysis. The V_P velocity difference between passive seismic and VSP was generally less than 15%, and about 5% in the area of interest. In turn, the V_P/V_S model correlated very well with the lithology derived by the VSP (Fig.11). Major geological

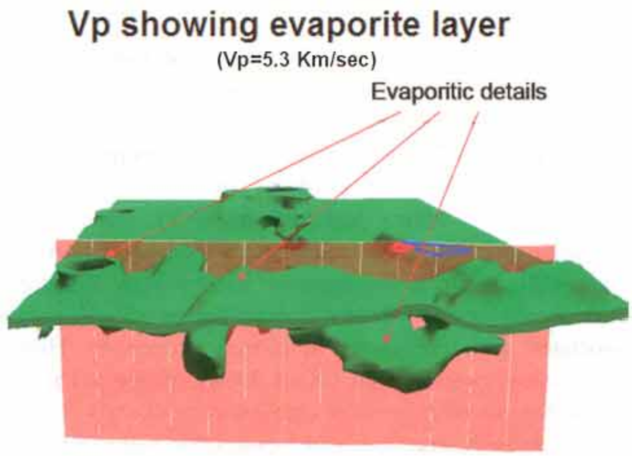

Figure 9 *Distribution of the evaporites.*

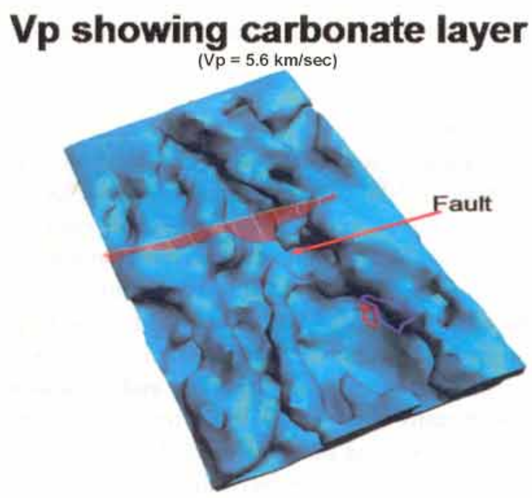

Figure 10 *Distribution of the carbonates.*

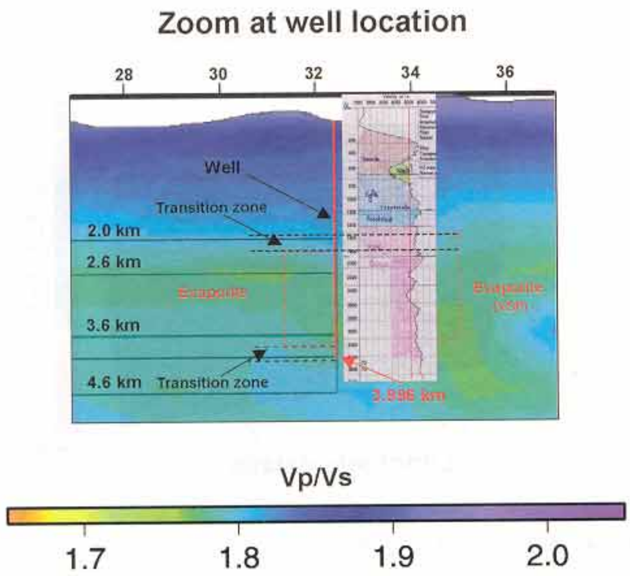

Figure 11 *V_P/V_S passive seismic tomography results around the well. A very good fit.*

formation boundaries around the well are, in fact, very close to the boundaries indicated in the passive model. This V_P/V_S volume (Poisson's ratio) ranges from 1.65 to 2.0. Low V_P/V_S values (1.65 - 1.75) were associated with evaporites and halite, high anhydrite (low porosity) content, and they correlate with lower density and high resistivity, matching the evaporitic properties predicted by other methods (Figure 6d). Cross-sections along the regional seismic lines indicate a clear, consistent and robust difference between V_P/V_S ranges associated with the above lithologies (Figure 8). Higher V_P/V_S values ranging from 1.8 - 1.9 were related to carbonate (higher porosity) layers of high velocity (V_P >5.6 km/sec), correlating with structural and topographic highs (Figs 7 & 10). More detailed comparison with well results suggest that high values of V_P/V_S are indicative of water-saturated zones that appear not only very near the surface, but also in fault zones and discontinuities (transition in Figure 11), correlating with high pressure water zones encountered in the well during drilling.

Conclusions

The 3D passive seismic tomography method was tested successfully in NW Greece to evaluate an exploration concession in a thrust belt. The results were detailed enough to contribute to the selection of a well location and proved to be superior to the regional 2D seismic results for a fraction of the cost. The main goal of the study was to obtain a coarse grid of the structural and lithologic characteristics of the area. However, higher accuracy and resolution could have been easily obtained if a larger number of stations, say 60 instead of 40, had been deployed. The decision to deploy more stations is usually project-driven, and such an increase in the number of stations would not affect the passive budget drastically.

This method has the potential to *replace some conventional land seismic*, at least in the exploration phase, provided enough micro-earthquakes occur in the first 10-20 km of the subsurface over the concession area. This may well be less of a problem than is commonly supposed; e.g. recent tests showed the Saudi Arabian Peninsula to be seismically active enough to justify the method, and there is no need for large seismic events!

In general terms the major conclusions from this study are:

- The passive seismic methodology has provided a cost-effective and environmentally friendly imaging tool, supporting expensive and often poor-quality seismic data.
- Results of this pioneering exploration tool have demonstrated that the technique could be useful not only in tectonically active regions, but also in other less active areas.
- Finally, confidence in the results (evaluated with well data) demonstrated the power of transmission tomography to provide accurate enough information not only for structural (V_P) but also lithologic (V_P/V_S) interpretation, often difficult to extract from conventional seismic.

Finally, extraction of information like focal mechanism, stress and moment tensor calculation related to fault geometry, fault generation mechanisms and fracture distribution, can be valuable for the estimation of reserves, well productivity, and possible drilling risks related to faults. Looking ahead, we are now ready to make use of passive seismic data beyond tomography, past exploration, and into delineation and even production studies.

References

Asad, A. M, J. N. Louie, and Pullammanappallil, S. K. [1994] Combination of linear inversion and nonlinear optimization for hypocenter and velocity estimation. *EOS Trans. Am. Geophys. Un.* 75, suppl. to no. 44 (Nov. 1), 425.

Eberhart-Phillips, D. [1993] Local earthquake tomography: earthquake source regions, in *Seismic Tomography Theory and Practice*, Iyer & Hirahara (eds), Chapman Hall, London.

Thurber, C.H. [1993] Local earthquake tomography: velocities and V_P/V_S-theory, in *Seismic Tomography Theory and Practice*, Iyer & Hirahara (eds), Chapman Hall, London.

Zhao, D. Hasegawa, A. and Horiuchi, S. [1992] Tomographic imaging of P and S wave velocity structure beneath NE Japan. *J.Geophys.Res.* 97, 19909-19928.

Acknowledgments

The authors and LandTech Enterprises would like to thank Enterprise Oil and partners for permission to publish the results of this study.